CrRb: a molecule with large magnetic and electric dipole moments

Z. Pavlović,[1,2,*] H. R. Sadeghpour,[1,†] R. Côté,[2,‡] and B. O. Roos[3,§]

[1]*ITAMP, Harvard-Smithsonian Center for Astrophysics, 60 Garden Street, Cambridge, Massachusetts 02138, USA*
[2]*Department of Physics, University of Connecticut, Storrs, Connecticut 06269-3046, USA*
[3]*Department of Theoretical Chemistry, University of Lund, S-221 00 Lund, Sweden*

(Dated: February 4, 2022)

We report calculations of Born-Oppenheimer potential energy curves of the chromium-rubidium heteronuclear molecule (^{52}Cr^{87}Rb), and the long-range dispersion coefficient for the interaction between ground state Cr and Rb atoms. Our calculated van der Waals coefficient ($C_6 = 1770$ a.u.) has an expected error of 3%. The ground state $^6\Sigma^+$ molecule at its equilibrium separation has a permanent electric dipole moment of $d_e(R_e = 3.34$ Å$) = 2.90$ D. We investigate the hyperfine and dipolar collisions between trapped Cr and Rb atoms, finding elastic to inelastic cross section ratio of 10^2–10^3.

PACS numbers: 34.20.-b,34.50.Cx

I. INTRODUCTION

The creation and manipulation of ultracold polar molecules in their ground state is a growing endeavor in atomic and molecular physics. Rubidium is the workhorse of ultracold atomic physics. It was the first atom to be Bose condensed and it remains a favorite atom for simulations of correlated and many-body physics, and for forming cold molecules. The chromium atom has also been Bose condensed and it is the only atomic species for which strong dipolar interaction has been observed [1]. Dipole moments, by virtue of their long-range $1/R^3$ interaction, where R is the separation between atoms, can be tuned by external fields with increasing precision to control atomic interactions with applications to precision measurements, molecular physics and information processing.

CrRb is a heteronuclear molecule, and may therefore possess a sizable permanent electric dipole moment. In its ground electronic state, it has magnetic moment of five Bohr magnetons ($5\mu_B$), so it can be magnetically tuned. In its most abundant form (84%), ^{52}Cr has no nuclear spin, $i = 0$, but its fermionic isotope ^{53}Cr (9.5% abundance) has nuclear spin, $i = 3/2$, that couples to electronic spin, $s = 3$, to produce a number of hyperfine levels. Therefore, bosonic-fermionic mixtures of CrRb can be formed with large electric and magnetic dipole moments, with potentially interesting applications for degenerate dipolar Fermi gases and spinor physics.

There is no spectroscopic information available for the CrRb molecule. A two-species magneto-optical trap (MOT) for Cr and Rb was realized in 2004 [2], in which some 4×10^6 ^{52}Cr atoms and 3×10^6 ^{87}Rb atoms were loaded. Cr is known to have large inelastic two-body spin-flip losses, so it cannot be maintained in a MOT [3, 4]. Owing to its large magnetic moment, magnetic trapping (MT) of Cr is possible [3], which allows the atoms to be trapped in its lowest high-field seeking state with total electronic spin $s = 3$ and its projection $m_s = -3$. In the Rb-MOT + Cr-MT configuration, Hensler *et al.*[2] measured the two-body loss rate constant to be $\beta_{\mathrm{RbCr}} \sim 1.4 \times 10^{-11}$ cm^{-3}/s and $\beta_{\mathrm{CrRb}} \sim 10^{-10}$ cm^{-3}/s, where the former refers to the loss due to the introduction of Cr into the Rb-loaded MOT, and the latter refers to loading of the Cr-MT first. The latter loss coefficient is about an order of magnitude larger than the former loss coefficient, because in the more shallow Cr-MT, interspecies dipolar interactions lead more quickly to spin depolarizing collisions, hence depletion of the trap.

In this *ab initio* work, we analyze the electrostatic interaction of Rb and Cr atoms in their ground states, obtain Born-Oppenheimer (BO) potential ground state energy curves, the long-range dispersion C_6 coefficient, and present a value for the electric dipole moment of the CrRb molecule. We use the resulting potential energy curves to calculate the elastic and relaxation cross sections, hyperfine and dipolar Fano-Feshbach resonances which can be used to tune the interactions.

II. NUMERICAL CALCULATIONS AND COLLISIONAL RESULTS

The calculations of the BO potential energy curves and the permanent electric dipole moments were performed with the multiconfiguration complete active space self-consistent field (CASSCF/CASPT2) method [5, 6]. The basis set was of VQZP quality with the primitives obtained from the relativistic ANO-RCC basis set ($7s6p4d3f2g1h$ for Cr and $8s7p4d2f1g$ for Rb)[7, 8]. Scalar relativistic effects are included in the calculations using the Douglas-Kroll-Hess Hamiltonian, as is standard in the MOLCAS software. Two active spaces were used. The first comprised the Cr $3d$ and $4s$ orbitals and the Rb $5s$, thus seven orbitals with seven active electrons. In the

*pavlovic@phys.uconn.edu
†hrs@cfa.harvard.edu
‡rcote@phys.uconn.edu
§deceased.

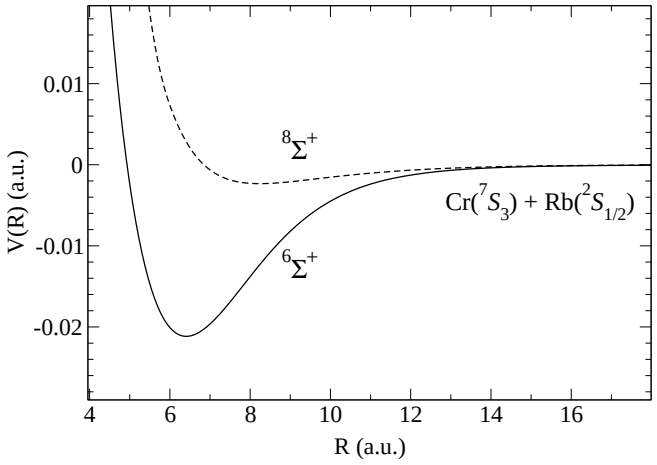

FIG. 1: The $^6\Sigma^+$ and $^8\Sigma^+$ potential energy curves for CrRb, correlating to Cr($^7S_3$) and Rb($^2S_{1/2}$) ground states.

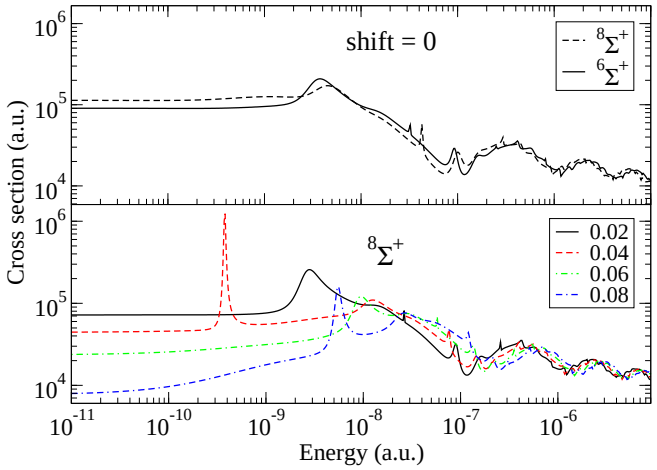

FIG. 2: (Color online) Top panel: Elastic cross section for the $^6\Sigma^+$ and $^8\Sigma^+$ curves without shift in the inner wall ($s = 0$). Bottom panel: Effect of the positive shifts on the elastic cross section along $^8\Sigma^+$ curve. Potential energy points for which $R < R_e$ are shifted according to $R_s = R + s(R - R_e)/(R_t - R_e)$, where s is the shift of the zero-energy classical inner turning point, R_t, and R_e is the equilibrium distance. Several different values for s were used.

second set of calculations, a second set of $3d$ orbitals was added to describe the $3d$ double shell effect: 12 orbitals with seven electrons. All calculations were performed with the MOLCAS-7 quantum chemistry software [9].

There are two electronic states which correlate to Rb ($6s\ ^2S$) and Cr($3d^5 4s\ ^7S$) ground states, $^6\Sigma^+$ and $^8\Sigma^+$. At large separation, R, these curves are well described by $-C_6/R^6$, where C_6 is the van der Waals (vdW) coefficient. We calculate C_6 using the Casimir-Polder [10] integral

$$C_6 = \frac{3}{\pi}\int_0^\infty \alpha_{\rm Cr}(i\omega)\alpha_{\rm Rb}(i\omega)d\omega, \qquad (1)$$

where the dynamic polarizability of each atom, $\alpha(i\omega)$, is given by

$$\alpha(i\omega) = \sum_\lambda \frac{f_{0\lambda}}{\epsilon_\lambda^2 + \omega^2}. \qquad (2)$$

The calculation of the dynamic polarizability requires knowledge of the oscillator strengths $f_{0\lambda}$ between the atomic ground state of energy ϵ_0 and atomic excited states of energy ϵ_λ. The summation is understood to also include integration over continuum. Our calculated value of C_6 for the Cr + Rb system, 1770 a.u., which we believe to be accurate within 3%, is obtained from the highly-accurate values of the Rb dynamic polarizability at imaginary frequencies [11] and the recently accurate values for the Cr dipole polarizability [12, 13]. This should be compared to the values of $C_6(\mathrm{Rb}_2) = 4691$ a.u. [10, 11], and $C_6(\mathrm{Cr}_2) = 770$ a.u., [4]. Both $^6\Sigma^+$ and $^8\Sigma^+$ curves share the same C_6 coefficient.

In Fig. 1, we plot the BO potential energy curves for CrRb in the ground electronic states. The equilibrium separation for the molecule in the ground state $^6\Sigma^+$ is $R_e = 6.31$ a.u. The value for the dipole moment at the equilibrium distance for the $^6\Sigma^+$ ground state molecule is $d_e = 2.90$ D (1.14 a.u.), which is reasonably large. The calculated static dipole polarizability for the molecule is $\alpha_{\rm CrRb}(0) = 701$ a.u. We should mention that $\alpha_{\rm Rb}(0) = 319$ a.u. [14] and $\alpha_{\rm Cr}(0) = 86$ a.u. [4]. The molecular value is 40% larger than the sum of atomic polarizabilities.

The dearth of spectroscopic and collisional information about the CrRb molecule limits what can be extracted from our calculations at ultracold temperatures. Nevertheless, we can inform the discussion by modifying the interaction potentials and evidence the changes to the phase shifts and/or cross sections at very low energies. Our vdW coefficient is sufficiently accurate to describe the potentials at large separations. In the short range repulsive wall region, we shift the potential energy curves, according to the prescription in our earlier work [12], and the results for the elastic cross sections are shown in Fig. 2. Several points can be made: while the cross sections are insensitive to the shifts for energies above $E \geq 10^{-8}$ a.u., they tend to decrease (increase) with increasing positive (negative) shifts at very low energies. However, when the shifts are large enough that an additional bound state (see for instance Fig. 3) is pulled in from the continuum, the above trend does not hold.

III. ZEEMAN CASCADE

The scattering between Cr and Rb atoms in the presence of a homogeneous magnetic field, $\boldsymbol{B}$, is governed by the following Hamiltonian

$$\hat{H} = -\frac{1}{2\mu R}\frac{\partial^2}{\partial R^2}R + \frac{\boldsymbol{l}^2}{2\mu R^2} + \hat{V}_{\rm es} + \hat{V}_{\rm dip} + 2\mu_B \boldsymbol{s}_{\rm A}\cdot\boldsymbol{B} + 2\mu_B \boldsymbol{s}_{\rm B}\cdot\boldsymbol{B} + A_{\rm hf}\boldsymbol{s}_{\rm B}\cdot\boldsymbol{i}_{\rm B}, \qquad (3)$$

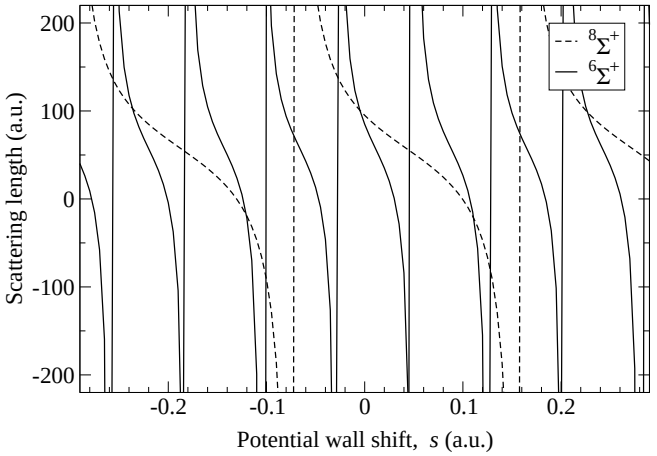

FIG. 3: The dependence of the energy of the last bound state in the $^6\Sigma^+$ and $^8\Sigma^+$ potentials on the shift parameter (s), see Fig. 2 for the shift definition. The "resonances" occur when an additional bound state is pulled in from the continuum as s decreases.

where the constants μ, μ_B and $A_{\rm hf}$ represent the reduced mass of the CrRb molecule, Bohr magneton, and Rb isotropic hyperfine interaction constant of the ground state, respectively. The first two terms in the Hamiltonian represent the nuclear kinetic energy of the molecule, where $\boldsymbol{l}$ is the rotational angular momentum of the nuclei. The explicit form of $\hat{V}_{\rm es}$, the operator of the electrostatic interaction, and $\hat{V}_{\rm dip}$, the operator of the magnetic dipolar interaction will be given below. The spin operators $\boldsymbol{s}_{\rm A}(\boldsymbol{i}_{\rm A})$ and $\boldsymbol{s}_{\rm B}(\boldsymbol{i}_{\rm B})$ represent the electronic (nuclear) spins of atom A (Cr) and atom B (Rb), respectively. For ^{52}Cr + ^{87}Rb system, the electronic and nuclear spins are $s_{\rm A} = 3$, $i_{\rm A} = 0$, $s_{\rm B} = 1/2$ and $i_{\rm B} = 3/2$ The linear atomic Zeeman terms and the isotropic hyperfine interaction for Rb are also given. The R-independent terms in the Hamiltonian (3), determine the scattering channels, which can be related through a unitary transformation $|\beta\rangle = \sum_\alpha U_{\beta\alpha}|\alpha\rangle$, to the product states of the total electronic spin, $\boldsymbol{S} = \boldsymbol{s}_{\rm A} + \boldsymbol{s}_{\rm B}$, and nuclear spin, $\boldsymbol{I} = \boldsymbol{i}_{\rm A} + \boldsymbol{i}_{\rm B}$, $|\alpha\rangle = |SM_SIM_I\rangle$. In this work, we neglect the interaction of the Rb nuclear magnetic moment with $\boldsymbol{B}$.

The total wave function expansion by product states of τ_{SM_S}, the eigenfunctions of $\boldsymbol{S}^2$ and $\boldsymbol{S}_z$, and τ_{IM_I}, the eigenfunctions of $\boldsymbol{I}^2$ and $\boldsymbol{I}_z$, is:

$$\Psi = \sum_{S,M_S}\sum_{I,M_I} G_{SM_SIM_I}(\boldsymbol{R})\tau_{SM_S}\tau_{IM_I}. \qquad (4)$$

We introduce channel wave functions, $G_{SM_SIM_I}(\boldsymbol{R})$, that describe the motion of the nuclei. Substitution of the expansion (4) in the Schrödinger equation leads to a system of coupled differential equations. A further simplification is achieved by introducing a set of channel wave functions that depend only on R,

$$G_{SM_SIM_I}(\boldsymbol{R}) = \sum_{l,m_l} F_{SM_SIM_Ilm_l}(R)Y_{lm_l}(\hat{\boldsymbol{R}}), \qquad (5)$$

where $\hat{\boldsymbol{R}}$ determines the direction of $\boldsymbol{R}$. The operator $\hat{V}_{\rm es}$ is defined in terms of the Born-Oppenheimer interaction potentials $V_S(R)$ for the CrRb molecule,

$$\hat{V}_{\rm es} = \sum_S \sum_{M_S} V_S(R)|SM_S\rangle\langle SM_S|. \qquad (6)$$

This decomposition makes the operator $\hat{V}_{\rm es}$ diagonal in the basis (4).

The magnetic dipolar operator [15], in the second rank irreducible tensor representation, can be written as

$$\hat{V}_{\rm dip} = -\sqrt{\frac{24\pi}{5}}\frac{\alpha^2}{R^3}\sum_{q=-2}^{2}(-1)^q Y^{(2)}_{-q}\left[\boldsymbol{s}_{\rm A}\otimes\boldsymbol{s}_{\rm B}\right]^{(2)}_q, \qquad (7)$$

where α is the fine-structure constant. The matrix of the dipolar interaction (7) can be evaluated analytically as demonstrated, for example, in [15, 16]. It is the only term in the Hamiltonian that can couple channel wave functions with different rotational numbers, l, according to

$$\Delta l = 0, \pm 2; \quad \text{while} \quad 0 \to 0 \quad \text{is forbidden.} \qquad (8)$$

A similar rule holds for the change of the total electronic spin of two atoms

$$\Delta S = 0, \pm 1, \pm 2. \qquad (9)$$

The dipolar interaction preserves the angular projections, M_I, and $M_S + m_l$ independently.

The Zeeman interaction term is $2\mu_0 BM_S$, where M_S is the projection of $\boldsymbol{S}$ on $\boldsymbol{B}$. The hyperfine interaction term can be directly evaluated in the coupled basis $|f_{\rm A}f_{\rm B}FM_F\rangle$, where $\boldsymbol{f}_{\rm A} = \boldsymbol{i}_{\rm A} + \boldsymbol{s}_{\rm A}$, $\boldsymbol{f}_{\rm B} = \boldsymbol{i}_{\rm B} + \boldsymbol{s}_{\rm B}$, and $\boldsymbol{F} = \boldsymbol{f}_{\rm A} + \boldsymbol{f}_{\rm B}$, and then through the chain of transformations

$$|f_{\rm A}f_{\rm B}FM_F\rangle \to |SIFM_F\rangle \to |SM_SIM_I\rangle, \qquad (10)$$

expressed in the $|SM_SIM_Ilm_l\rangle$ basis. The hyperfine interaction matrix elements are calculated as in [17, 18].

The highest low-field seeking state is chosen as the initial channel for the Zeeman relaxation of maximally stretched Cr and Rb atoms. In this state, the spin numbers for ^{52}Cr are $f = 3$ and $m_f = 3$, while for ^{87}Rb the relevant spin numbers are $f = 2$ and $m_f = 2$. The results do not change much when we exclude states which represent the decrease of the total spin projection, M_F, by more than 2 units. Figure 4(a) contains the cross sections as a function of energy at three values of B. The cross sections display characteristic dipolar shape resonances, and roughly correspond to cross sections for Cr-Cr scattering scaled down 10 times. The inelastic cross section contribution from the dipolar interaction scales as [19]

$$\frac{\sigma_{inel}^{\rm CrRb}}{\sigma_{inel}^{\rm CrCr}} \sim \left(\frac{s_{\rm Rb}}{s_{\rm Cr}}\right)^{3/2}\left(\frac{\mu_{\rm CrRb}}{\mu_{\rm CrCr}}\right)^2. \qquad (11)$$

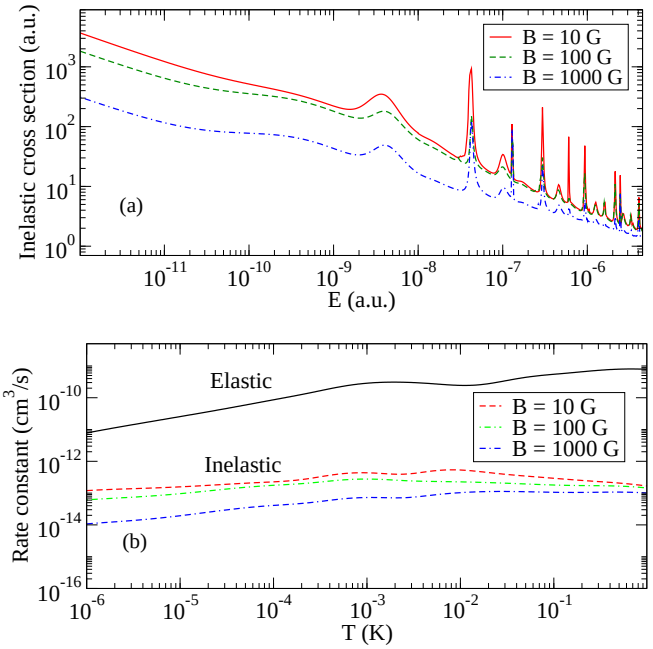

FIG. 4: (Color online) (a) Energy dependence of inelastic cross section for the relaxation of maximally stretched ^{52}Cr, $|f{=}3, m_f{=}3\rangle$, and ^{87}Rb, $|f{=}2, m_f{=}2\rangle$, atoms in the presence of magnetic field. (b) Rate constants for elastic and inelastic scattering processes presented in (a).

The Zeeman relaxation rates, Fig. 4(b), provide a valuable tool in assessing the efficiency of CrRb evaporative cooling in a magnetic or optical trap. Ratios of elastic to inelastic collisions in the μK regime of about 100−1000 times are possible.

In CrRb, we have an interesting system where strong hyperfine and dipole-dipole interactions compete to produce rich spectra. When only the hyperfine interaction in ^{87}Rb is considered, the scattering length dependence with the magnetic field, Fig. 5 (bottom panel) shows a number of hyperfine-coupled Fano-Feshbach resonances, where the initial state is the lowest high-field seeking state, $|^{52}\mathrm{Cr} : f{=}3, m_f{=}{-}3;\ ^{87}\mathrm{Rb} : f{=}1, m_f{=}1;\ l{=}0, m_l{=}0\rangle$. When the Cr magnetic dipole interaction with the spin of the Rb atom is "turned on", the much richer spectrum (top panel in Fig. 5) is obtained, where the additional resonances, due to the dipolar interaction, have (s, d) wave character.

In summary, we calculate the $^6\Sigma^+$ and $^8\Sigma^+$ BO potential energy curves of CrRb in the ground electronic state, the long-range C_6 vdW coefficient, the static molecular polarizability, and the equilibrium permanent electric dipole moment. We obtain the spin relaxation rate constants for collision of Cr and Rb in a magnetic field and investigate the magnetic tunability of the scattering length in the presence of hyperfine and dipolar interactions. With its relatively large electric and magnetic dipole moments, CrRb is a potentially interesting molecule for collisional studies of dipolar molecules in combined electric and magnetic fields. With fields at different angles, it may be possible to tune the two dipoles into cooperative or competitive arrangement.

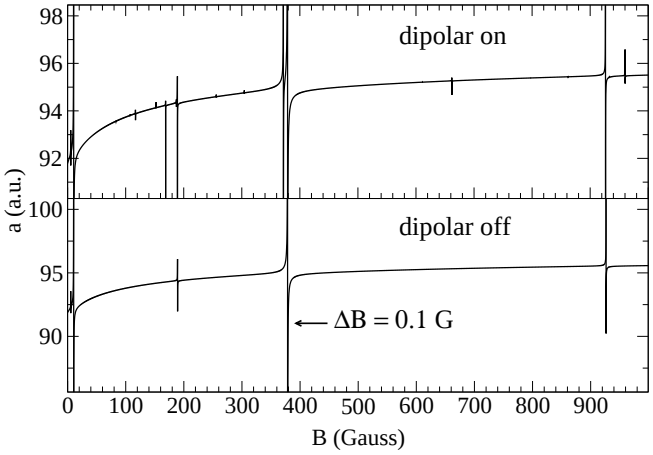

FIG. 5: Competing hyperfine and dipolar interactions in the $l = 0$ entrance channel state: $|f{=}3, m_f{=}{-}3\rangle$ for ^{52}Cr, and $|f{=}1, m_f{=}1\rangle$ for ^{87}Rb. Bottom panel: Resonances caused by Rb hyperfine interaction, Top panel: Effect of dipolar interaction coupling entrance s-wave channel to the closed d-wave channels.

ACKNOWLEDGMENTS

This work was supported by a grant from the NSF to ITAMP. The work of Z.P. and R.C. was partially supported by grant PHY-0653449 of the NSF.

[1] A. Griesmaier, J. Werner, S. Hensler, J. Stuhler, and T. Pfau, Phys. Rev. Lett. **94**, 160401 (2005); Q. Beaufils, R. Chicireanu, T. Zanon, B. Laburthe-Tolra, E. Marechal, L. Vernac, J. C. Keller, and O. Gorceix, Phys. Rev. A **77**, 061601(R) (2008).
[2] S. Hensler, A. Griesmaier, J. Werner, A. Görlitz, and T. Pfau, J. Mod. Opt. **51**, 1807 (2004).
[3] J. Stuhler, P. O. Schmidt, S. Hensler, J. Werner, J. Mlynek, and T. Pfau, Phys. Rev. A **64**, 031405 (2000); C. C. Bradley, J. J. McClelland, W. R. Anderson, and R. J. Celotta, Phys. Rev. A **61**, 053407 (2000).
[4] Z. Pavlović, R. V. Krems, R. Côté, and H. R. Sadeghpour, Phys. Rev. A **71**, 061402(R) (2005).
[5] B. O. Roos, "The complete active space self-consistent field method and its applications in electronic structure calculations," in *Advances in Chemical Physics; Ab Ini-*

tio Methods in Quantum Chemistry - II, edited by K. P. Lawley (John Wiley & Sons Ltd., Chichester, England, 1987), Chap. 69, p. 399.

[6] K. Andersson, P.-Å. Malmqvist, and B. O. Roos, J. Chem. Phys. **96**, 1218 (1992).

[7] B. O. Roos, V. Veryazov, and P.-O. Widmark, Theor. Chim. Acta **111**, 345 (2004).

[8] B. O. Roos, R. Lindh, P.-Å. Malmqvist, V. Veryazov, and P.-O. Widmark, J. Phys. Chem. A **109**, 6575 (2005).

[9] G. Karlström, R. Lindh, P.-Å. Malmqvist, B. O. Roos, U. Ryde, V. Veryazov, P.-O. Widmark, M. Cossi, B. Schimmelpfennig, P. Neogrady, and L. Seijo, Comput. Mater. Sci. **28**, 222 (2003).

[10] M. Marinescu, H. R. Sadeghpour, and A. Dalgarno, Phys. Rev. A **49**, 982 (1994).

[11] A. Derevianko, W. R. Johnson, M. S. Safranova, and J. F. Babb, Phys. Rev. Lett. **82**, 3589 (1999).

[12] Z. Pavlović, R. V. Krems, R. Côté, and H. R. Sadeghpour, Phys. Rev. A **69**, 030701(R) (2004).

[13] J. Werner, A. Griesmaier, S. Hensler, J. Stuhler, T. Pfau, A. Simoni, and E. Tiesinga, Phys. Rev. Lett. **94**, 183201 (2005).

[14] R. W. Molof, H. L. Schwartz, T. M. Miller, and B. Bederson, Phys. Rev. A **10**, 1131 (1974)

[15] R.V. Krems and A. Dalgarno, J. Chem. Phys. **120**, 2296 (2004)

[16] A. M. Arthurs and A. Dalgarno, Proc. Phys. Soc. London A, **256**, 540 (1960).

[17] T. V. Tscherbul, P. Zhang, H. R. Sadeghpour, and A. Dalgarno, Phys. Rev. A **79**, 062707 (2009).

[18] R. N. Zare, *Angular Momentum—Understanding Spatial Aspects in Chemistry and Physics* (John Wiley & Sons, Inc., New York, 1988).

[19] S. Hensler, J. Werner, A. Griesmaier, P.O. Schmidt, A. Görlitz, T. Pfau, S. Giovanazzi, K. Rzazewski, Appl. Phys. B **77**, 765 (2003).